

TOWARDS AN EXPLANATION OF THE SPACE STAR ANOMALY*

A. WILCZEK

for the Few-Body Systems Collaboration

Institute of Physics, University of Silesia, 41-500 Chorzów, Poland

(Received January 22, 2018)

One of the most intriguing discrepancies observed in the proton–deuteron breakup reaction is known as the Space Star Anomaly. The effect was found to peak at the energies ranging from 7.5 to 13 MeV/nucleon, but due to scarcity of data at higher energies, it has not been explained yet. Recently, a new analysis has been started in order to fill the gaps in our understanding of the problem. As the first step, the differential cross sections were calculated on the basis of the CD-Bonn potential, including explicit Δ excitation (coupled-channel potential) as well as the Coulomb force, in order to identify the effects that may contribute to the cross sections. The calculations were done for $d(160 \text{ MeV})+p$, $p(108 \text{ MeV})+d$ and $p(135 \text{ MeV})+d$ breakup reactions.

DOI:10.5506/APhysPolB.49.457

1. Introduction

Few-body systems play an important role of a fundamental laboratory in the research on nuclear interactions. The system of three nucleons ($3N$) is of special importance, as the simplest non-trivial environment, in which the nucleon–nucleon (NN) interaction models can be tested. Although the NN interactions play a dominant role in the few-nucleon interactions, there are several theoretical investigations that point to an existence of additional dynamical effects — three-nucleon force ($3NF$). It emerges in systems composed of at least three nucleons.

Nowadays, two theoretical approaches in modelling the dynamics of $3N$ systems are prevalent. Since, for the energies of interest, it is not possible to apply QCD to the calculations directly, nucleons and pions are used as effective degrees of freedom. In the first approach, phenomenological NN

* Presented at the XXXV Mazurian Lakes Conference on Physics, Piaski, Poland, September 3–9, 2017.

potentials are combined with an additional 3NF model (or the Δ isobar is included in an explicit way, like in the case of the Coupled Channels (CC) method [1, 2]). The other approach is more fundamental and it applies the Chiral Perturbation Theory in order to reach an Effective Field Theory description (Chiral EFT) [3, 4]. Recent developments of the calculations with realistic potentials involve relativistic effects [5–7] as well as Coulomb interactions [8].

Even though the development of the theories is well advanced, some experimentally observed effects have not been explained yet. The discrepancies between the theory and the experiment were observed both in cross sections and in polarisation-dependent observables. The most intriguing inconsistencies are *e.g.* the A_y puzzle (for analysing powers) and the Space Star Anomaly (SSA). The latter effect is quite astonishing as the problems with description of cross sections usually appear at relatively high energies, while the SSA marks its presence at low energies. The effect has not been explained theoretically since its discovery in 1989 [9].

Investigations of deuteron breakup in a specific star configuration brought some interesting results to light [9–14]. The configuration is defined in the centre-of-mass system as a final state, where the momenta of the outgoing nucleons are of the same value, and the angle between them equals 120° . Depending on the angle of inclination with respect to the beam axis (α), one distinguishes between Space Star for $\alpha = 90^\circ$, Forward Plane Star ($\alpha = 0^\circ$) and Backward Plane Star ($\alpha = 180^\circ$).

Analysis of the $^1\text{H}(d, pp)n$ reaction shows the biggest discrepancies for the Space Star configuration at energies ranging from 7.5 to 13 MeV/nucleon, where the differences reach 15% [10], and the theories overestimate the measurements. The main component of the theoretical cross sections at such low energies results from the s-wave channel of the $2N$ interaction. This reduces the range of possible explanations for the effect. The predicted 3NF effects and the Coulomb interactions between protons are very small and they were taken into account in the calculation without clarifying the observed inconsistency. Relativistic effects are negligible there and cannot make such a large contribution to the effect. Up till now, it was also not possible to reach a reliable description of the SSA in ChEFT.

Another unexpected effect is observed for the Space Star configuration at low energies, where a charge asymmetry between the cross sections for deuteron on neutron breakup (the experimental cross sections exceed theoretical predictions by 30% [12, 15]) and deuteron on proton breakup (on the contrary — the experimental cross sections are 15% below the calculated ones) is visible. A set of very precise and accurate cross-section measurements for breakup, in both $p + d$ and $n + d$ interactions in a wide range of energies, is needed to solve this charge-symmetry breaking puzzle.

2. Experimental data at medium energies

There are some data sets collected in $d + p \rightarrow p + p + n$ experiments with the use of large acceptance detectors in the range of medium energies. So far, they have not been analysed with respect to the star configurations. The aim of this project is to obtain cross sections for the star configurations in the $^1\text{H}(d, pp)n$ breakup reaction at deuteron energies of 50 and 160 MeV/nucleon. The data will be analysed as a function of the angle α between the beam momentum vector and the decay plane. The results will be compared with the predictions of the most recent models of the three-nucleon forces.

Moreover, new measurements are being performed in order to obtain the cross sections for $^2\text{H}(p, pp)n$ breakup at the proton beam energy of 108, 135, and 160 MeV. The measurements are carried out at the Cyclotron Centre Bronowice, Institute of Nuclear Physics, Polish Academy of Sciences in Kraków.

The BINA detector, used for these studies, consists of a scattering chamber equipped with a liquid deuterium target system. The detection system is divided into two parts: the Ball, surrounding the target and built out of 149 polyhedral plastic scintillators, and the Wall. The Wall is used for registering particles at forward angles. Their tracks are reconstructed based on the charge detected in a MultiWire Proportional Chamber, which consists of 3 detection layers. The ΔE hodoscope works in combination with the energy detectors as a particle identification system. If a particle is detected by the Ball, the averaging over angular acceptance of each element of the Ball has to be taken into account in the analysis. BINA covers a solid angle of almost 4π , what makes the system well-suited for measurements of the Space Star geometry.

3. Theoretical predictions

The existing and new data collected with the BINA detector will be analysed with respect to the star configurations. Below, we discuss which configurations can be extracted from those data and what dynamical effects (3NF, Coulomb interaction) are expected to play an important role. In Table I, the centre-of-mass angles are translated into the laboratory frame angles for each beam type (proton, deuteron) and energy. The theoretical predictions for the star configurations in the three reactions investigated with the BINA experimental setup ($d(160 \text{ MeV})+p$, $p(108 \text{ MeV})+d$, and $p(135 \text{ MeV})+d$) were calculated. Three configurations were studied for each energy: Forward Plane Star (FPS: $\alpha = 0^\circ$), Space Star ($\alpha = 90^\circ$), and Backward Plane Star (BPS: $\alpha = 180^\circ$).

TABLE I

Polar (θ_1, θ_2) and relative azimuthal ϕ_{12} angles of protons in the laboratory frame for the star configurations of different α (Forward Plane Star, Space Star, Backward Plane Star) calculated using relativistic kinematics.

Reaction	α	$\theta_1 = \theta_2$	ϕ_{12}
$p(108 \text{ MeV})+d$	0	34.82	180
	90	53.55	120
	180	74.99	180
$p(135 \text{ MeV})+d$	0	34.73	180
	90	53.45	120
	180	74.93	180
$d(160 \text{ MeV})+p$	0	23.49	180
	90	34.15	120
	180	42.19	180

In order to investigate the expected strength of 3NF and Coulomb effects, three models were compared for each configuration: CD-Bonn with Coulomb potential (CDB+C), CD-Bonn with explicit Δ excitation (CDB+ Δ), and CD-Bonn with both Δ and Coulomb (CDB+ Δ +C) [8]. The two latter potentials include 3NF, whereas the former is a pure 2NF potential. A cut at 20 MeV was applied on theoretical data to take into account the experimental threshold for protons registered with the BINA detector. The BPS configuration for $p(108 \text{ MeV})+d$ is completely rejected by this cut, as all the kinematics is below the threshold.

The results are presented in Fig. 1, where polar angles and relative azimuthal angle of the protons in the laboratory frame are equal to those of the star configurations. The graph is plotted against the length of kinematics (S). The points on the symmetry axis correspond to the configuration, for which the energies of the outgoing protons are equal (the star configuration). When moving away from the symmetry axis, the configuration becomes more and more asymmetric (momenta differ from each other). The solid line stands for CDB+C, dashed line for CDB+ Δ , and dotted line for CDB+ Δ +C potential (3NF). The ratios of the predictions of each of the two former models to those of the latter are also presented for comparison. A cut on proton energy of 20 MeV was applied.

The results show that the strongest effect for $d(160 \text{ MeV})+p$ is caused by 3NF, although it is not very prominent (2–5% for the star configurations). On the other hand, for the $p+d$ reaction at both energies (108, and 135 MeV), the FPS configuration shows a significant influence of the Coulomb force (8–10%), whereas the effects of 3NF are minimal. 3NF increases with α and

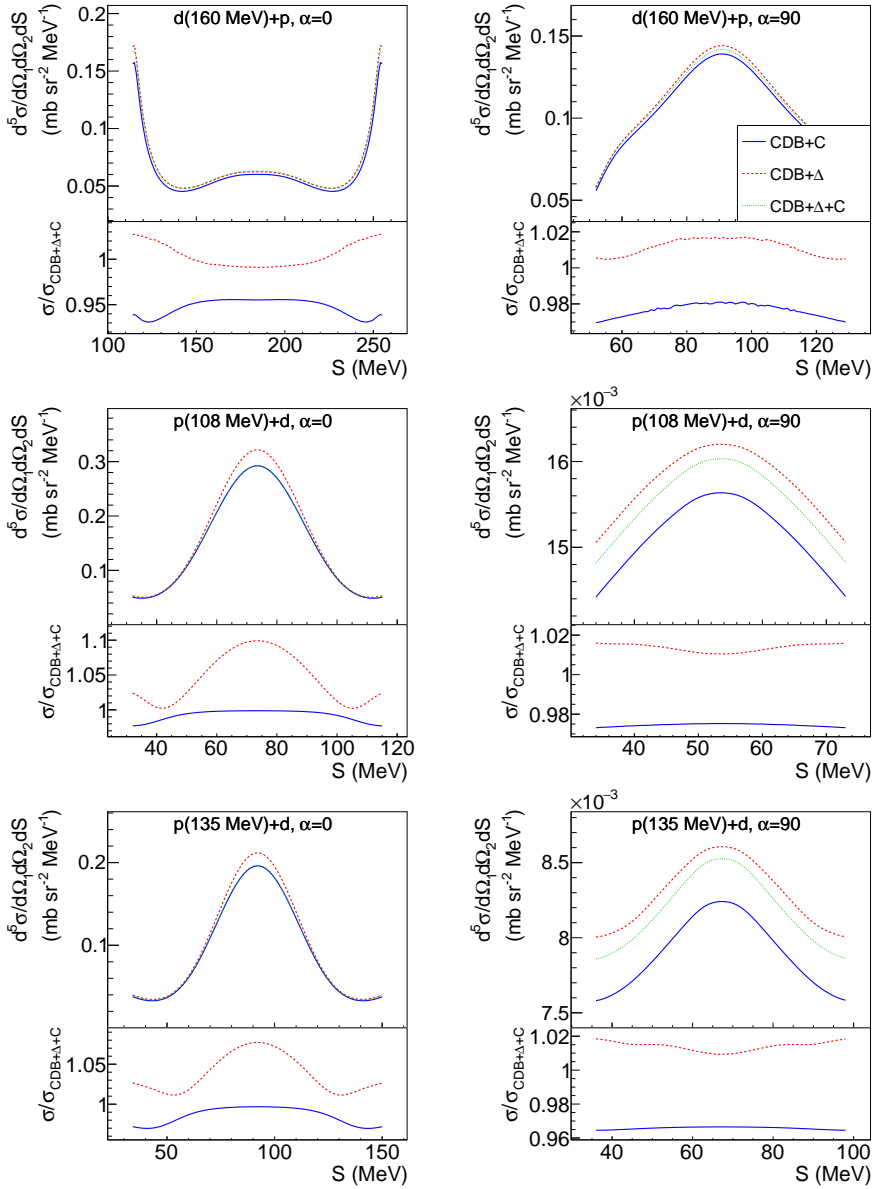


Fig. 1. Cross sections for breakup configurations plotted against the length of kinematics (S). The star configurations correspond to the symmetry axis of the plot. Ratios of the cross sections calculated with the CDB+ Δ and CDB+C potentials to the results obtained for the full CDB+ Δ +C potential are shown in the bottom panels.

has the most prominent effect on the cross sections for BPS. The 3NF effect for the analysed star configurations generally tends to increase the cross section. Coulomb force effects are negligible, except for FPS in the case of $d+p$.

Since there are no calculations including all dynamical ingredients (3NF, Coulomb and relativistic effects), the predicted low influence of 3NF and Coulomb force is favourable when searching for any ‘anomalies’ in the data measured for the star configurations. On the other hand, it was shown that relativistic effects play a major role in the description of Space Star at 65 MeV [5]. It is expected that their contribution becomes larger at higher energies [5–7], so such effects should be easy to separate from anomalies prevalent at low energies.

The data will be compared with the cross sections being measured by the BINA@CCB experiment in order to look for deviations from the theoretical predictions including Coulomb force and 3NF effects. The models restricting the role of those are auxiliary and will be used for troubleshooting if any discrepancy occurs.

This project is supported by the National Science Centre, Poland (NCN) (grants No. 2016/23/D/ST2/01703 and 2012/05/B/ST2/02556). The author would like to thank A. Deltuva for preparations of scattering amplitudes and the cross-section software.

REFERENCES

- [1] P.U. Sauer, A. Deltuva, R. Machleidt, *Phys. Rev. C* **68**, 024005 (2003).
- [2] P.U. Sauer, A. Deltuva, K. Chmielewski, *Phys. Rev. C* **67**, 034001 (2003).
- [3] U.-G. Meißner *et al.*, *Phys. Rev. C* **66**, 064001 (2002).
- [4] W. Glöckle, U.-G. Meißner, E. Epelbaum, *Eur. Phys. J. A* **19**, 125 (2004).
- [5] H. Witała, J. Golak, R. Skibiński, *Phys. Lett. B* **634**, 374 (2006).
- [6] H. Witała, *Phys. Rev. C* **83**, 044001 (2011).
- [7] R. Skibiński, H. Witała, J. Golak, *Eur. Phys. J. A* **30**, 369 (2006).
- [8] A. Deltuva, *Phys. Rev. C* **80**, 064002 (2009).
- [9] J. Strate *et al.*, *Nucl. Phys. A* **501**, 51 (1989).
- [10] K. Ohnaka *et al.*, *Few-Body Syst.* **55**, 725 (2014).
- [11] K. Sagara *et al.*, *Few-Body Syst.* **48**, 59 (2010).
- [12] K. Sagara, *Few-Body Syst.* **55**, 1073 (2014).
- [13] K. Ishibashi *et al.*, *Few-Body Syst.* **54**, 295 (2013).
- [14] J. Zejma *et al.*, *Phys. Rev. C* **55**, 42 (1997).
- [15] Z. Zhou *et al.*, *Nucl. Phys. A* **684**, 545 (2001).